TECHNICAL MEMORANDUM
X-222

STATIC LONGITUDINAL STABILITY CHARACTERISTICS OF A BLUNTED GLIDER REENTRY CONFIGURATION HAVING 79.5° SWEEPBACK AND 45° DIHEDRAL AT A MACH NUMBER OF 6.2 AND ANGLES OF ATTACK UP TO 20°

By Edward E. Mayo

Langley Research Center
Langley Field, Va.

CLASSIFIED DOCUMENT - TITLE UNCLASSIFIED

NATIONAL AERONAUTICS AND SPACE ADMINISTRATION
WASHINGTON
October 1959

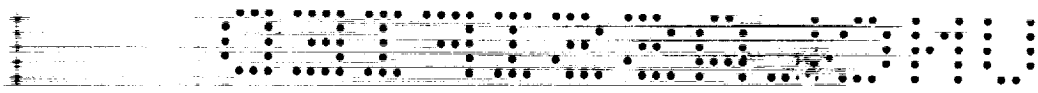

code 1

copy #1

NATIONAL AERONAUTICS AND SPACE ADMINISTRATION

TECHNICAL MEMORANDUM X-222

STATIC LONGITUDINAL STABILITY CHARACTERISTICS OF A BLUNTED GLIDER REENTRY CONFIGURATION HAVING 79.5° SWEEPBACK AND 45° DIHEDRAL AT A MACH NUMBER OF 6.2 AND ANGLES OF ATTACK UP TO 20°*

By Edward E. Mayo

SUMMARY

An experimental investigation was conducted at a Mach number of 6.2 to determine the static longitudinal stability characteristics of a model of a blunted glider reentry configuration having 79.5° sweepback and 45° dihedral. The free-stream Reynolds number for the investigation was 3.0×10^6 based on the basic model length of 7.5 inches. Tests were made through an angle-of-attack range from 0° to 20° (with respect to the ridge line) at zero sideslip only. The investigation showed that incorporating 10° nose incidence in the basic model resulted in a lower lift-curve slope, a lower lift-drag ratio, a higher value of trim lift coefficient, and a decrease in static longitudinal stability. In comparison, the effect of extending the configuration length and incorporating 10° and 20° boattail angles resulted in smaller changes in the longitudinal stability characteristics of the model.

INTRODUCTION

At present there is considerable need for aerodynamic data on various winged, manned, reentry configurations. This report deals with experimental static longitudinal stability characteristic data obtained at a Mach number of 6.2 on a blunted glider reentry configuration having 79.5° sweepback and 45° dihedral. The model was very similar to the configuration conceived from heat-transfer considerations in reference 1. The low-speed stability investigation (ref. 2) showed that the configuration of reference 1 had essentially linear pitching and lateral characteristics at low angles of attack. Pressure measurements on the configuration at a Mach number of 4.95 are given in reference 3.

Presented herein are lift, drag, and pitching-moment data obtained on the model in the Langley Gas Dynamics Laboratory at a Mach number of

*Title, Unclassified.

6.2, a test-section Reynolds number of 3.0×10^6 based on the basic model length of 7.5 inches, and an angle-of-attack range from 0° to 20° (with respect to the ridge line).

SYMBOLS

The data are referred to the wind axes. (See fig. 1.) The moments are measured with respect to the center of gravity of the basic model. The coefficients are based on the projected plan-form area and the mean aerodynamic chord of the basic model.

b	wing span, in.
c	chord, in.
$\bar{c}$	mean aerodynamic chord of basic model $\dfrac{\int_0^{b/2} c^2 dy}{\int_0^{b/2} c\, dy}$, in.
C_D	drag coefficient, $\dfrac{D}{qS}$
C_L	lift coefficient, $\dfrac{L}{qS}$
C_m	pitching-moment coefficient, $\dfrac{M_Y}{qS\bar{c}}$
$(C_L)_{trim}$	lift coefficient at trim
C_{L_α}	lift-curve slope, rate of change of lift coefficient with angle of attack, per deg
C_{m_α}	pitching-moment-curve slope, rate of change of pitching-moment coefficient with angle of attack, per deg
D	drag, lb
L	lift, lb
$\left(\dfrac{L}{D}\right)_{max}$	maximum lift-drag ratio

l	length of basic model, in.
l_N	length of inclined nose section, in.
M	free-stream Mach number
M_Y	pitching moment, in-lb
q	free-stream dynamic pressure, lb/sq in.
S	projected plan-form area of basic model, sq in.
$\frac{x_{np}}{\bar{c}}$	location of neutral point, fraction of mean aerodynamic chord $\left(0.45 - \frac{dC_m}{dC_L}\right)$
y	lateral coordinate, in.
α	angle of attack of bottom of model (ridge line), deg

MODELS AND CENTER-OF-GRAVITY LOCATION

Five configurations were investigated. Drawings of the configurations are presented in figure 2, and a photograph of each configuration tested is given in figure 3. The dimensional characteristics are as follows:

Airfoil section	10.7° wedge
Wing area, sq in.	15.92
Span (to rounded edges), in.	3.54
Aspect ratio	0.79
Root chord, in.	7.5
Tip chord, in.	0
Mean aerodynamic chord, in.	5.83
Sweepback of leading edge, deg	79.5
Dihedral, deg	45
Boattail extension, in.	0.90
Nose radius (between ridge line and flat surface), in.	0.11
Ridge-line radius, in.	0.55
Leading-edge radius, in.	0.055

The basic model (figs. 2(a) and 3(a)) had triangular cross sections with rounded edges, 45° dihedral lower surfaces, and a flat upper surface.

The sweep of the leading edge measured in the plan form was 79.5°. The model with 20° boattail (figs. 2(b) and 3(b)) consisted of the basic model with the addition of a 20° boattail whose length was 12 percent of the basic model length. The boattail angle was measured from the plane of the model surface as is shown in figure 2. The model with 10° boattail consisted of the model with 20° boattail with the addition of 10° wedges on the 20° boattail. (See figs. 2(c) and 3(c).) The model with 0° boattail consisted of the model with 20° boattail with the addition of 20° wedges on the 20° boattail. (See figs. 2(d) and 3(d).) The model with nose incidence (figs. 2(e) and 3(e)) had the same geometry as the basic model except that the nose $\left(\frac{l_N}{l} = 0.267\right)$ was inclined 10°.

All the configurations were constructed of aluminum with the exception of the model with nose incidence, which was constructed of cherry wood. The cherry wood did not char during the test run. Figure 3(e) shows a photograph of the model with nose incidence after the test.

The longitudinal center-of-gravity position was taken as $0.45\bar{c}$ and to a vertical position on a line connecting the centroid of the base with the apex. The $0.45\bar{c}$ position was arrived at from the results of reference 2, which indicated neutral stability on a very similar model for low speeds. In order to be consistent with reference 2, the longitudinal axis was chosen parallel to the ridge line as shown in figure 1. The basic model center-of-gravity location (see fig. 2) was used as the origin of the axes for all configurations tested.

APPARATUS AND TESTS

The tests were conducted in the Langley Gas Dynamics Laboratory at $M = 6.2$ at a stagnation pressure of 315 pounds per square inch absolute and a stagnation temperature of 450° F. These conditions correspond to a free-stream Reynolds number of 4.8×10^6 per foot or 3.0×10^6 based on the model length of 7.5 inches. Tests were made through an angle-of-attack range from 0° to 20° at zero sideslip only.

At each angle of attack, force measurements were made by means of a sting-supported, internal, electrical strain-gage balance. The balance and model rotated on the angle-of-attack mechanism.

The axial force was corrected to the condition of free-stream static pressure acting on the base area. Base pressures were determined from measurements obtained from a 1/8-inch-diameter tube attached to the outside of the balance shield housing and projecting to within 1/16 inch of the base for each configuration tested. It was assumed that the pressure measured acted over the entire base.

The test repeatability was very good as indicated by repeat runs (flagged symbols in figs. 4(a) and 4(b)).

RESULTS AND DISCUSSION

The variation of pitching-moment coefficient, drag coefficient, and angle of attack with lift coefficient for the models is given in figure 4. A detailed discussion of the results of the investigation is not attempted in this paper; however, the results of most interest are presented in the following table:

Configuration	Figure	C_{L_α} $(C_L = 0)$	C_L at $\left(\frac{L}{D}\right)_{max}$	$\left(\frac{L}{D}\right)_{max}$	$\frac{x_{np}}{\bar{c}}$	$(C_L)_{trim}$	C_{m_α}
Basic model	4(a)	0.015	0.12	2.8	0.55	0.022	-0.0015
Model with 20° boattail	4(b)	.015	.14	2.7	.56	.017	-.0017
Model with 10° boattail	4(c)	.016	.14	2.9	.60	.017	-.0025
Model with 0° boattail	4(d)	.017	.16	2.9	.63	.008	-.0031
Model with nose incidence	4(e)	.013	.14	2.3	.49	[a].3	-.0006

[a]Extrapolated data.

A comparison of the test results given in figure 4 shows that all configurations tested have essentially linear variations of pitching-moment coefficient with lift coefficient for the angle-of-attack range investigated.

The static longitudinal stability $\left(C_{m_\alpha}\right)$ decreased as the boattail angle increased. This corresponds to a decrease in lift rearward of the center of gravity as the boattail angle increased. As would be expected, incorporating nose incidence on the basic model resulted in the most forward location of the neutral point for all models tested.

The maximum lift-drag ratio for the investigation ranged from 2.3 to 2.9 and occurred at angles of attack between 14° and 17°. Only small changes in $\left(\frac{L}{D}\right)_{max}$ with model extension and boattail angle were observed, whereas $\left(\frac{L}{D}\right)_{max}$ was reduced about 18 percent when nose incidence was incorporated.

The value of $(C_L)_{trim}$ for all models with the exception of the model with nose incidence corresponds to an angle of attack of about 7°. The trim lift coefficient for the model with nose incidence corresponds to an angle of attack of approximately 28°.

The model with 10° nose incidence has the lowest C_{L_α}, the lowest $\left(\frac{L}{D}\right)_{max}$, the most forward neutral-point location, and the highest value of $(C_L)_{trim}$.

CONCLUDING REMARKS

An experimental investigation was conducted at a Mach number of 6.2 to determine the static longitudinal stability characteristics of a model of a blunted glider reentry configuration having 79.5° sweepback and 45° dihedral. The investigation showed that incorporating 10° nose incidence in the basic model resulted in a lower lift-curve slope, a lower lift-drag ratio, a higher value of trim lift coefficient, and a decrease in static longitudinal stability. In comparison, the effect of extending the configuration length and incorporating 10° and 20° boattail angles resulted in smaller changes in the longitudinal stability characteristics of the model.

Langley Research Center,
National Aeronautics and Space Administration,
Langley Field, Va., July 28, 1959.

REFERENCES

1. Cooper, Morton, and Stainback, P. Calvin: Influence of Large Positive Dihedral on Heat Transfer to Leading Edges of Highly Swept Wings at Very High Mach Numbers. NASA MEMO 3-7-59L, 1959.

2. Paulson, John W.: Low-Speed Static Stability and Control Characteristics of a Model of a Right Triangular Pyramid Reentry Configuration. NASA MEMO 4-11-59L, 1959.

3. Cooper, Morton, and Gunn, Charles R.: Pressure Measurements on a Hypersonic Glide Configuration Having 79.5° Sweepback and 45° Dihedral at a Mach Number of 4.95. NASA TM X-223, 1959.

Figure 1.- Sketch of axis system. Arrows indicate positive direction.

(a) Basic model.

Figure 2.- Model geometry. Dimensions are in inches.

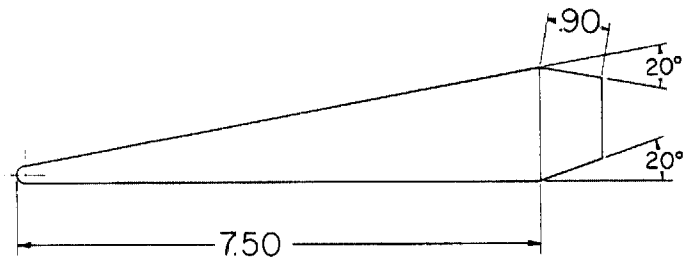

(b) Model with 20° boattail.

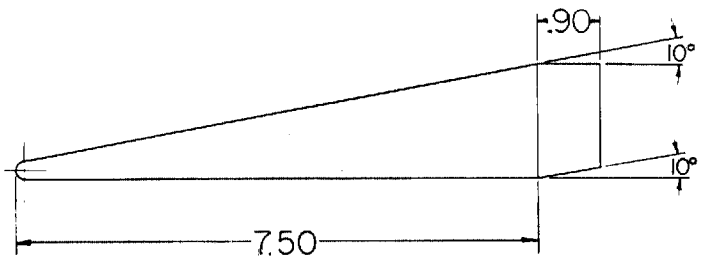

(c) Model with 10° boattail.

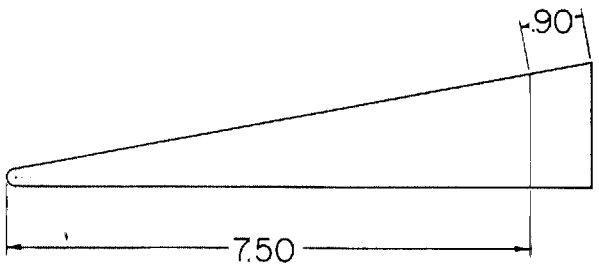

(d) Model with 0° boattail.

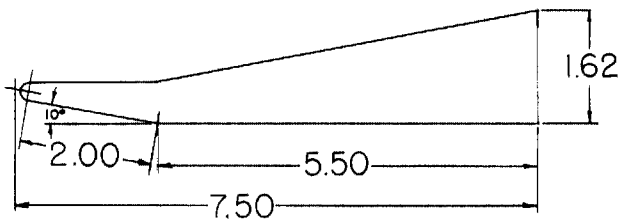

(e) Model with 10° nose incidence.

Figure 2.- Concluded.

CONFIDENTIAL

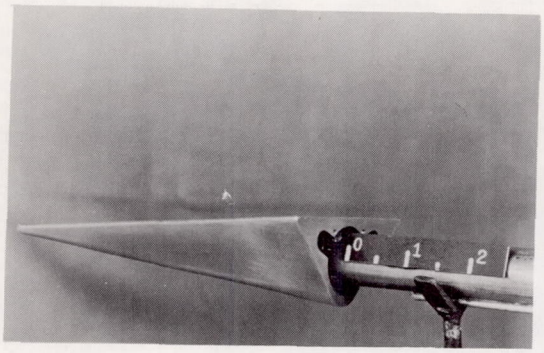

(a) Basic model.

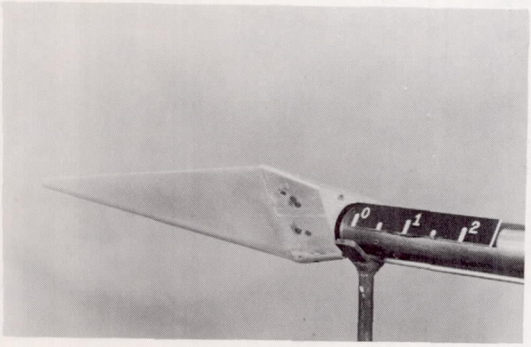

(b) Model with 20° boattail.

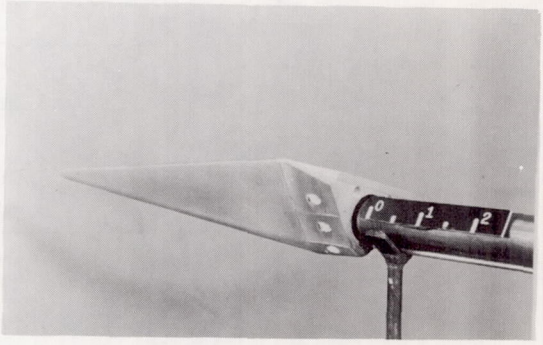

(c) Model with 10° boattail.

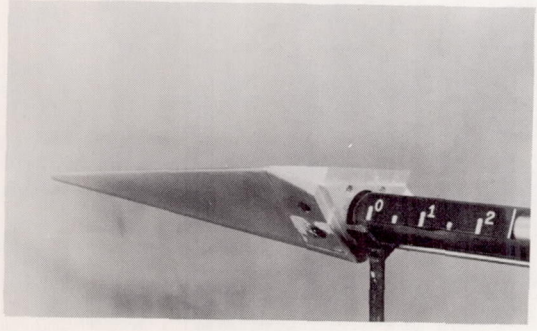

(d) Model with 0° boattail.

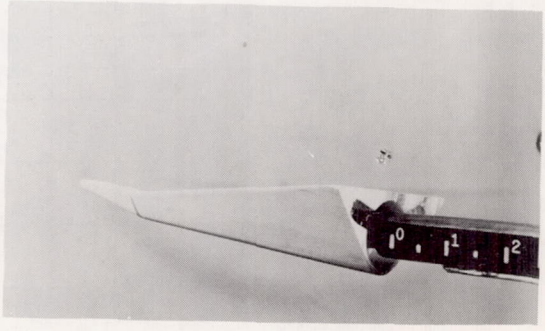

(e) Model with 10° nose incidence.

Figure 3.- Photographs of configurations investigated. L-59-5006

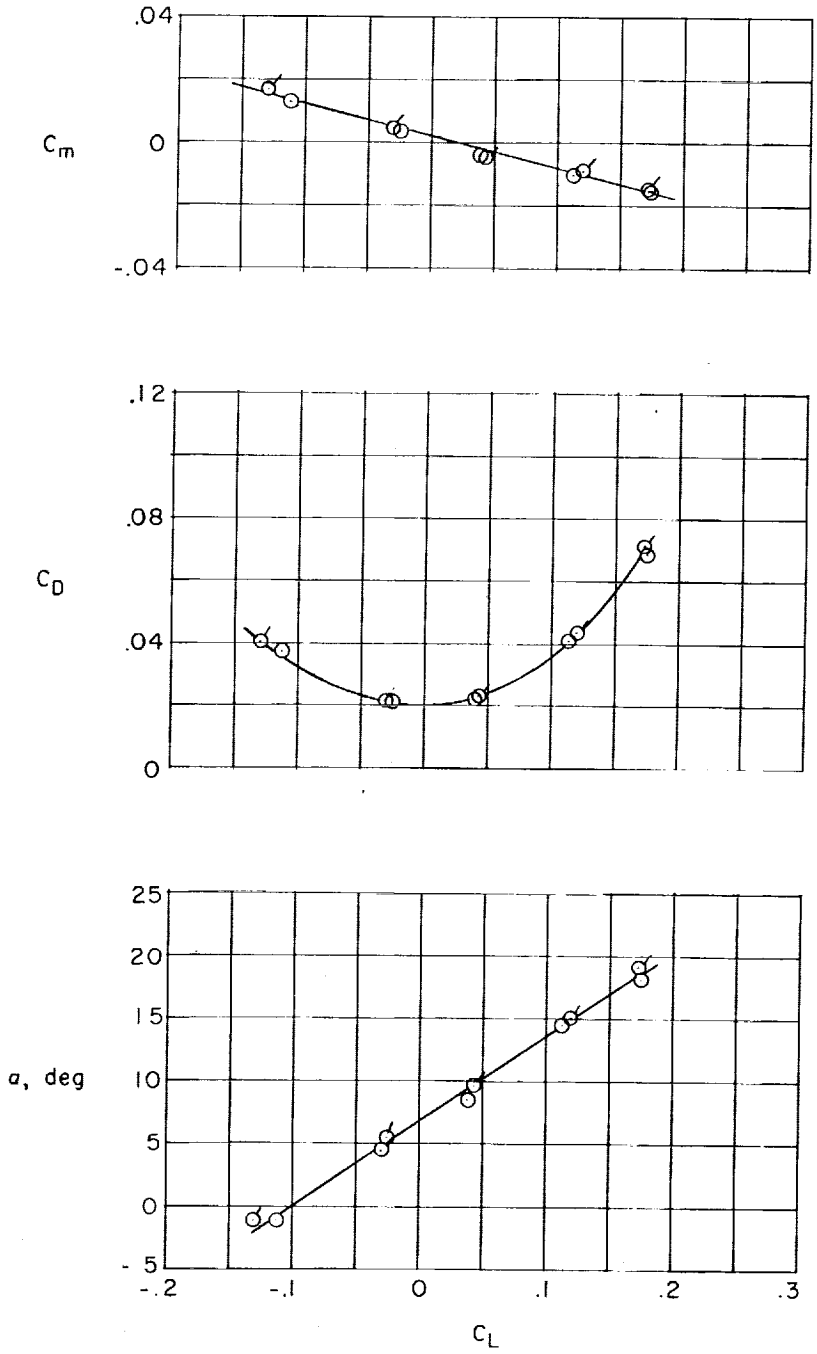

(a) Basic model.

Figure 4.- Longitudinal characteristics of model at M = 6.2. Flagged symbols indicate repeat runs.

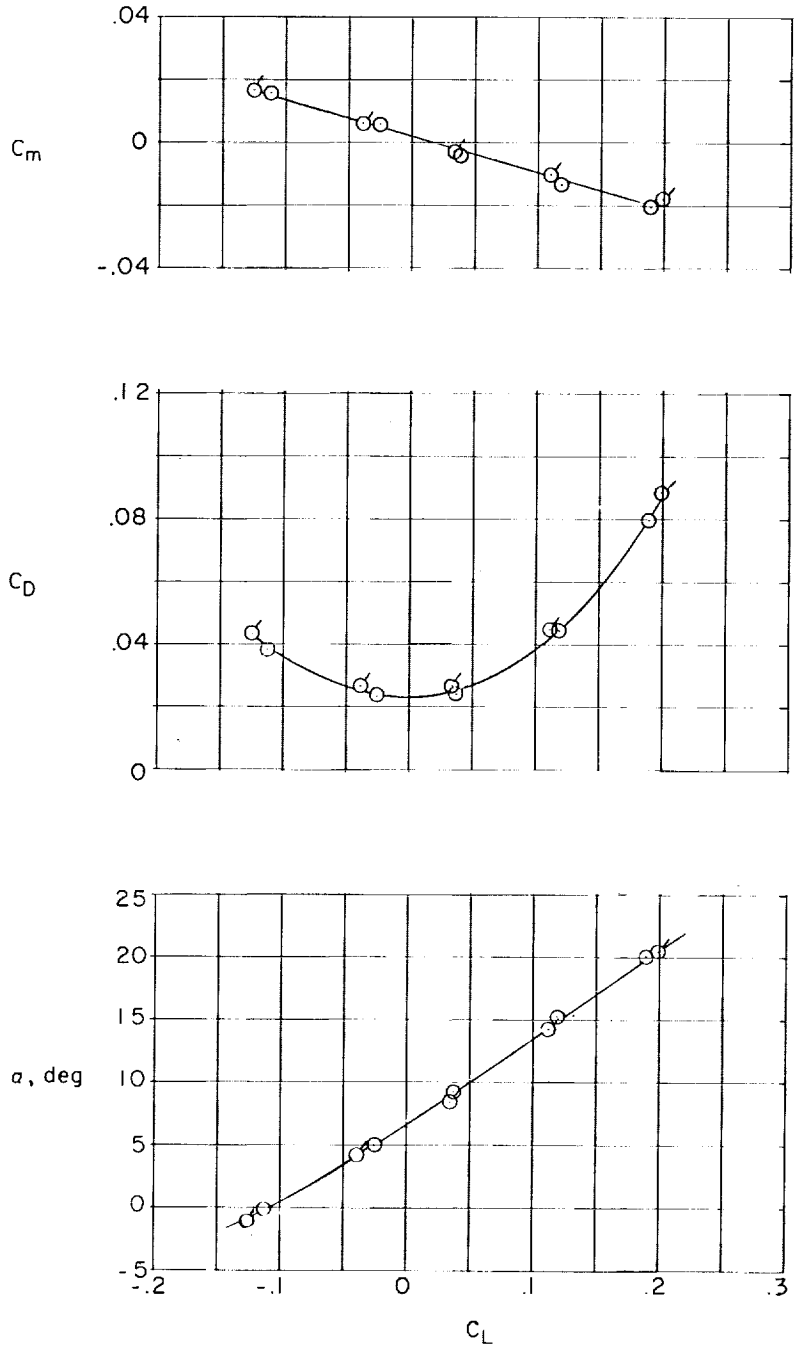

(b) Model with 20° boattail.

Figure 4.- Continued.

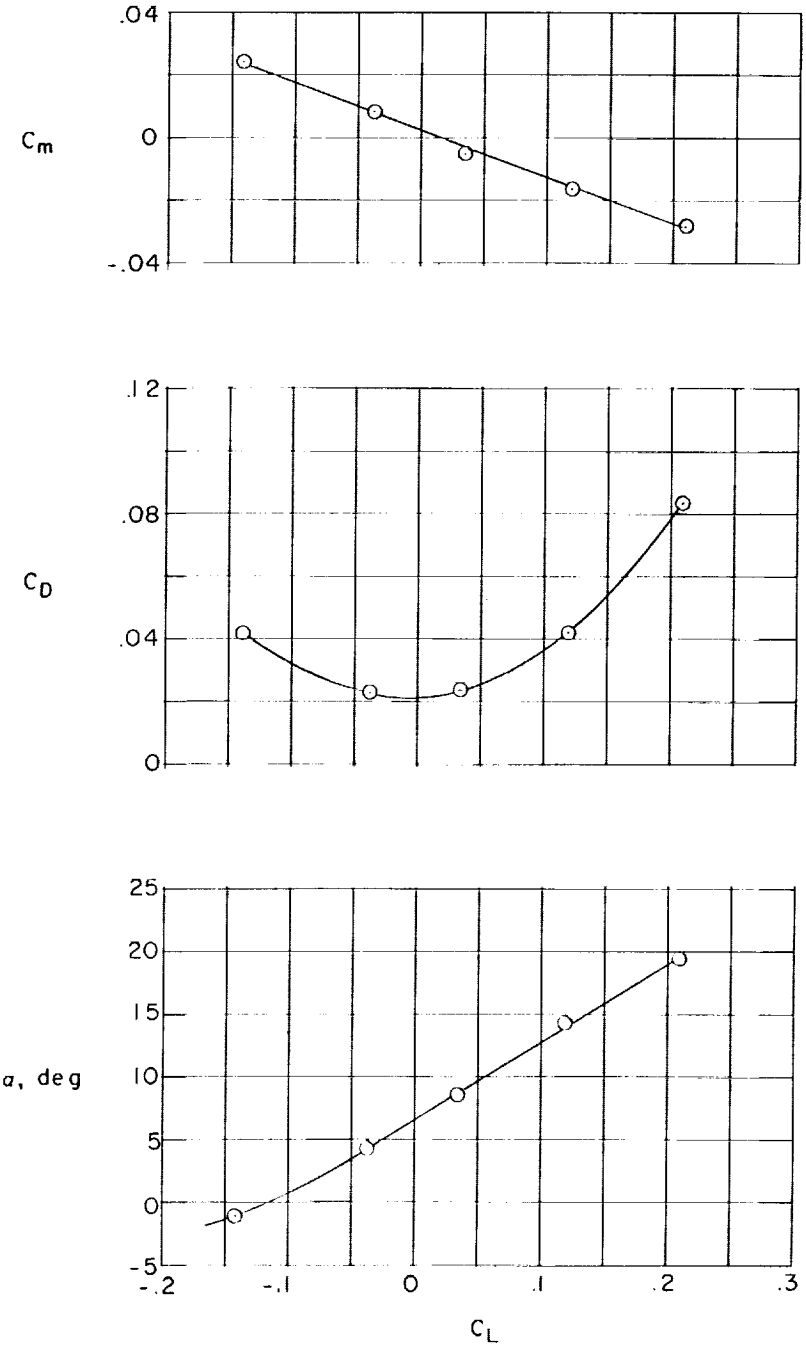

(c) Model with 10° boattail.

Figure 4.- Continued.

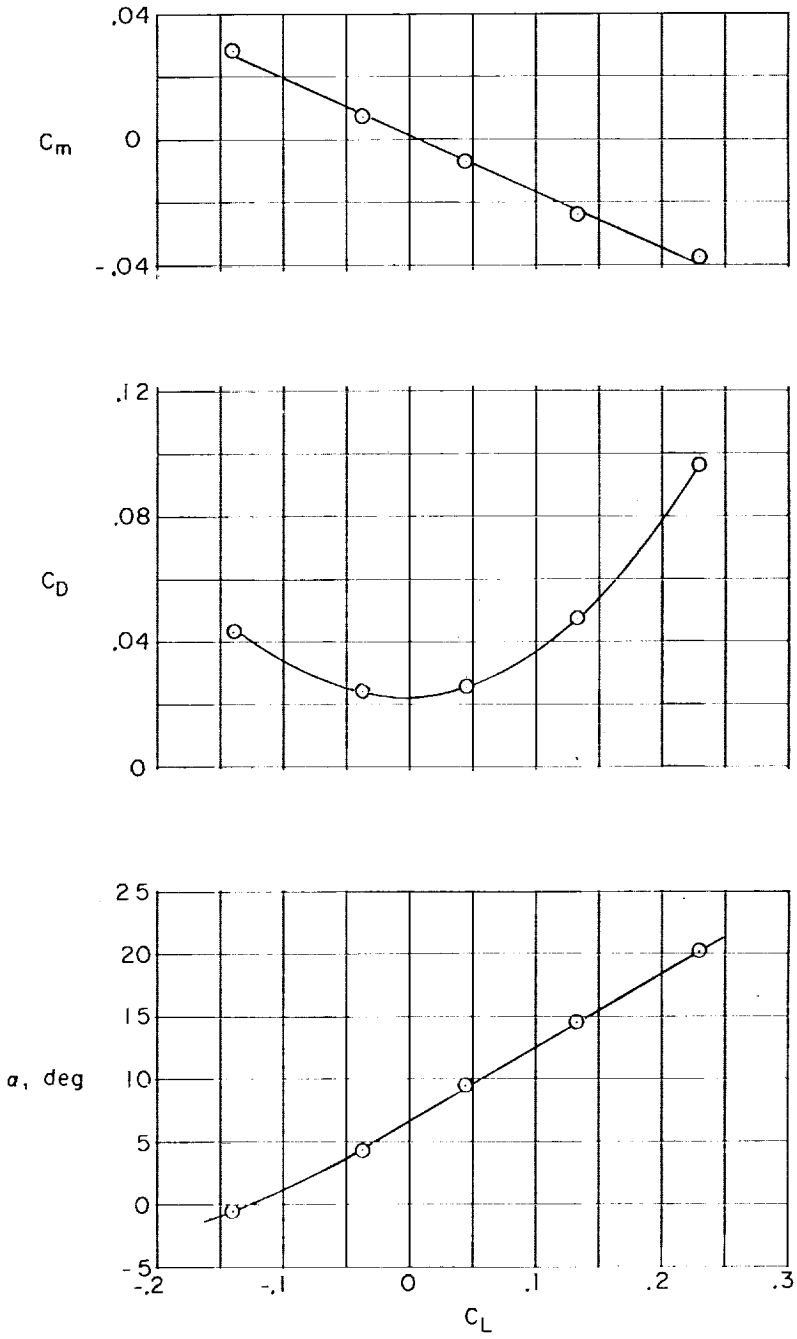

(d) Model with 0° boattail.

Figure 4.- Continued.

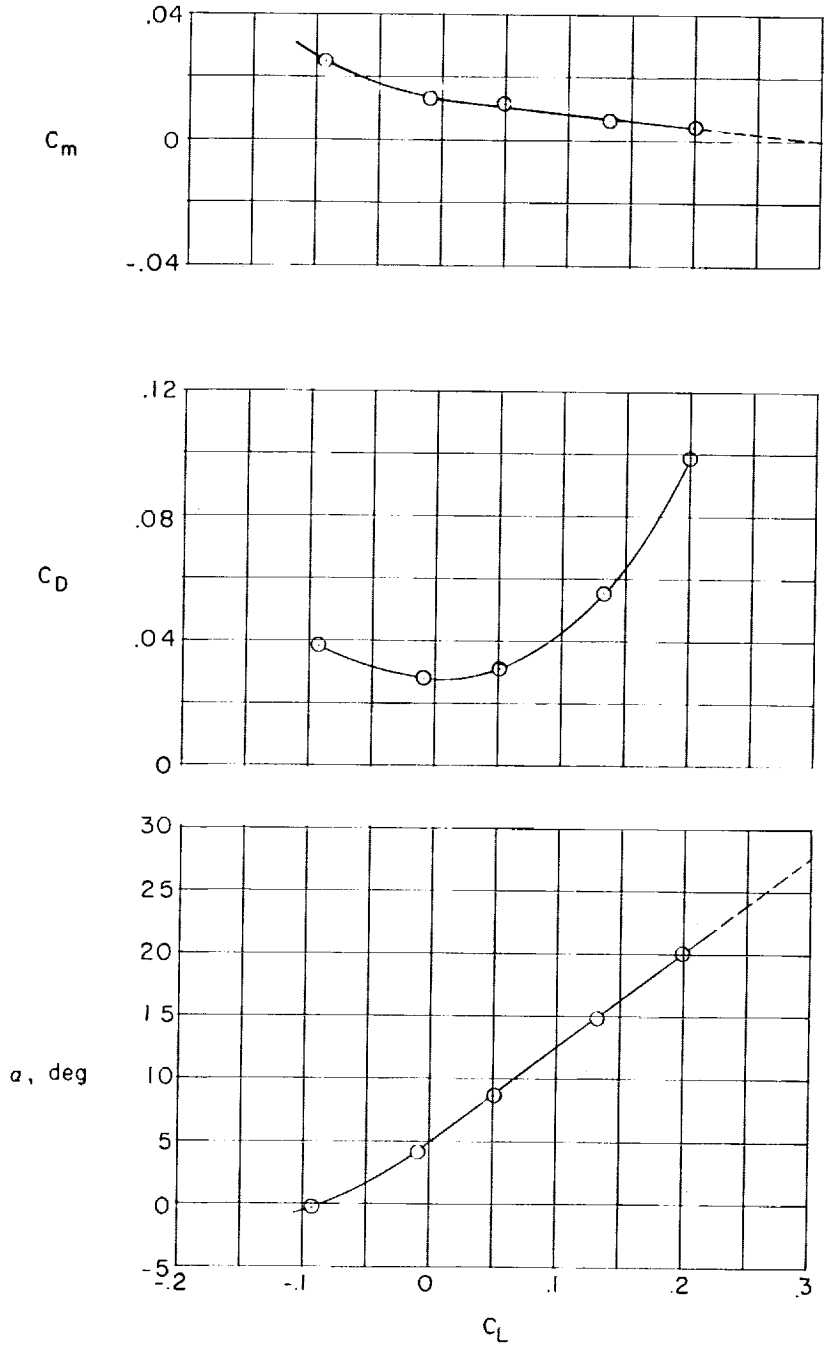

(e) Model with 10° nose incidence.

Figure 4.- Concluded.